

Porphyrin Binding and Irradiation Promote G-quadruplex DNA Dimeric Structure

Valeria Libera,^{1,2,3} Elena A. Andreeva,⁴ Anne Martel,⁵ Aurelien Thureau,⁶ Marialucia Longo,⁷ Caterina Petrillo,¹ Alessandro Paciaroni,¹ Giorgio Schirò,^{4,*} Lucia Comez^{3,*}

¹Dipartimento di Fisica e Geologia, Università di Perugia, 06123 Via Pascoli, Perugia, Italy

²Niels Bohr Institute, University of Copenhagen, Universitetsparken 5, 2100 Copenhagen, Denmark

³CNR-IOM c/o Dipartimento di Fisica e Geologia, Università di Perugia, 06123 Via Pascoli, Perugia, Italy

⁴Univ. Grenoble Alpes, CNRS, CEA, IBS, F-38000 Grenoble, France

⁵Institut Laue-Langevin - 71 avenue des Martyrs, 38042 GRENOBLE Cedex 9, France

⁶Swing Beamline, Synchrotron SOLEIL, Gif sur Yvette, France

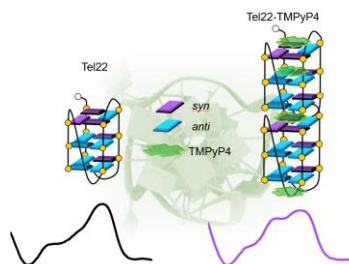
⁷Jülich Centre for Neutron Science at Heinz Maier-Leibnitz Zentrum, Lichtenbergstraße 1, 85748 Garching, Germany

Corresponding Authors: Email: comez@iom.cnr.it, giorgio.schiro@ibs.fr

ABSTRACT Nucleic acid sequences rich in guanines can organize into non-canonical DNA G-quadruplexes (G4s) of variable size. The design of small molecules stabilizing G4s' structure is a rapidly growing area to develop novel anticancer therapeutic strategies and bottom-up nanotechnologies. Among a multitude of binders, porphyrins are very attractive due to their light activation that can make them valuable G4s *conformational regulators*. Here, a structure-based strategy, integrating complementary probes, is employed to study the interaction between TMPyP4 porphyrin and a 22-base human telomeric sequence (Tel22) before and after irradiation with blue light. Porphyrin binding is discovered to promote Tel22 dimerization, while light irradiation of the Tel22-TMPyP4 complex controls the dimer fraction. Such a change in quaternary structure is found to be strictly correlated with modifications at the secondary structure level, thus providing

an unprecedented link between the degree of dimerization and the underlying G4s conformational changes.

TOC GRAPHICS



Porphyrin binding fosters Tel22 dimerization. Such a change at the quaternary structure-level is found to be strongly linked to modifications of the secondary structure, as revealed by circular dichroism spectroscopy.

KEYWORDS G-quadruplex • Porphyrin • Small-angle techniques • Circular Dichroism • Dimerization.

G-Quadruplexes (G4s) are non-canonical DNA structures formed by single-stranded sequences rich in guanines (G).¹ These motifs shaping up from G-tetrads stacked on top of each other, are stabilized by monovalent cations (in the order $K^+ > Na^+ > Li^+$) and connected by looping bases.^{2,3,4} A G-tetrad is a cyclic hydrogen-bonded square planar alignment of four guanines, with the guanines adopting either *anti* or *syn* alignments about glycosidic bonds. G4s are highly polymorphic structures,⁵ able to take a multitude of different topologies according to the possible combinations of guanine runs directions, as well as variations in loop size and sequences.^{6,7,8,9,10} The high degree of polymorphism together with conformational switching properties enable G4s structural reconfiguration and promote their applications in sensing, analytical biochemistry and

logic gate development.^{11,12} G4s are also of strategic importance in molecular biology and biomedicine^{13,14} since they are found throughout the genome and are overexpressed in the promoter regions of some oncogenes.

Remarkably, in such a context, it was shown that the ligand-induced stabilization of DNA quadruplexes inhibits the telomerase action and the proliferation of cancer cells.^{1,15–17,18} This is the reason why interaction of small molecules with G4s is a rapidly emerging strategy in the field of anticancer therapeutics.¹⁹ Among a reservoir of macrocyclic ligands, porphyrins are the most widely used for G4s. Due to both their shape and size (~ 9 Å side, comparable to that of an individual G tetrad, Figure 1a), they have indeed high affinity for several quadruplexes.^{20,21} In this work, we selected the archetypal TMPyP4 porphyrin, known for its ability to downregulate the expression of genes by quadruplex formation or induction in their promoter region.^{22,23,24} Its biological behavior was also studied against a broad variety of tumor cell lines.^{25,26–29}

When irradiated, porphyrins generate singlet oxygen (¹O₂), a property largely used in photodynamic therapy.^{30,31,32} In particular, it was recently shown that, in the interaction with G4s, singlets preferentially oxidize guanines at the exterior faces, sprouting numerous radicals and generating, as major end-product, spiroiminodihydantoin.³³ These products can promote splitting of external tetrads and subsequent structural rearrangements. Further, it was suggested that light-induced selective oxidation of the external guanines leads to a reduced telomerase activity in carcinogenic cells thus promoting telomere shortening.³⁴ Therefore, creating new knowledge on the effect of the interaction between G4s and porphyrins under light exposure will be fundamental for improving the use of porphyrin derivatives³² in phototherapy, where a reactive oxygen is needed to elicit the death of diseased cells.³⁵ We propose here a strategy to investigate the structure and interaction between TMPyP4 and the human telomeric sequence AG₃(TTAG₃)₃ (Tel22) in

presence of K^+ ions (Figure 1b), both in the dark and upon irradiation with blue light. The rationale of using a K^+ solution is its biological relevance due to the high intracellular concentration of K^+ (~140 mM).³⁶ Under these conditions, Tel22 is a mixture of two (3+1) hybrid-type (H) and basket-type topologies;³⁷ complexation with small molecules may significantly alter the equilibrium of these two different conformers.^{38,39,40,41,42,43}

Our method consists of combining X-ray and neutron small-angle scattering (SAXS and SANS) techniques with circular dichroism (CD) and UV-VIS absorption spectroscopy, commonly employed to characterize the secondary structure of biological materials. The goal is to explore the effect of light irradiation on the structure of the Tel22-TMPyP4 complex. The experimental set-up for light irradiation is described in the S.I. (Figure S1).

In order to study the binding of TMPyP4 to Tel22, we first measured absorption spectra in the UV-visible region of an 80 μ M solution of TMPyP4 as a function of Tel22 concentration, the latter ranging from 4 to 120 μ M (Figure 1c). The results clearly show an effect of hypochromicity in the Soret band (~422 nm) up to ~62% and a red-shift of ~15 nm (Figure 1d).^{44,45} The fraction of bound porphyrin was estimated from the change in the ligand absorption at 422 nm (see S.I. for details). Based on the spectroscopic titration described in Figure 1, and according to the saturation plot (Figure 1d), we selected a 1:2 Tel22/TMPyP4 ratio for SAXS/SANS and CD experiments.

SAXS was used to study the structural effect of porphyrin complexation before and after irradiation at 430 nm (Figure 2a). SAXS measurements were complemented by analogous SANS data (Figure 2b) in order to exclude any X-ray radiation effect on DNA and porphyrin. The pair-distance distribution function, $P(r)$, was calculated using the GNOM program from the ATSAS package,⁴⁶ and showed the impact of Tel22-TMPyP4 complexation (Figure 3a).

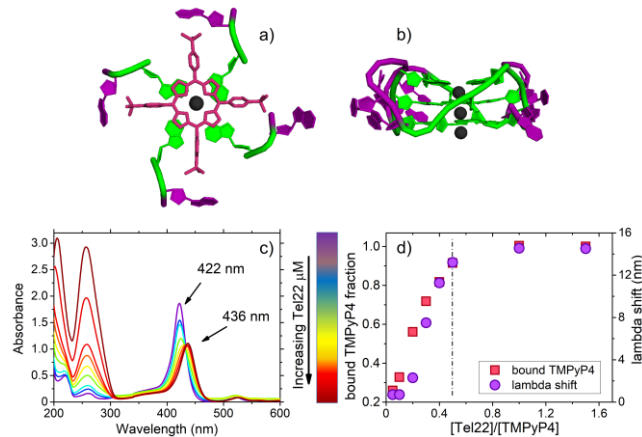


Figure 1. Spectroscopic titration. a) Qualitative superposition of TMPyP4 (red structure) and a G-tetrad (green and purple structure, extracted from PDB entries: 1KF1⁴⁷ and 2A5R⁴⁸) with a K⁺ ion (dark green sphere); b) Tel22 from PDB entry: 1KF1; c) UV-VIS absorption spectra of TMPyP4 as a function of Tel22 concentration; d) red-shift of the Soret band and fraction of bounded TMPyP4. Concentrations of Tel22 range from 4 μM to 120 μM, while TMPyP4 is kept at the fixed amount of 80 μM. The dashed line indicates the 1:2 Tel22/TMPyP4 ratio used for CD and SAXS/SANS experiments.

Before complexation, Tel22 is in a monomeric condition, as evidenced by the determination of a narrow single feature on the $P(r)$, similarly to what found by in the human telomeric hybrid-2 form 2JSL,⁴⁹ measured at comparable DNA concentration. The increase of $I(0)$ in the scattering curves together with the appearance of a shoulder above 40 Å on the $P(r)$, witnesses the dimerization of Tel22 into elongated structures. The process is then enhanced upon irradiation.

A fitting procedure in terms of monomers and dimers^{38,39,50} (Figure 3b and Figure S2) revealed the formation of Tel22 dimers upon binding that count for the ~60 % of the total population (further details are provided in the S.I.). Irradiation at 430 nm at increasing exposure times progressively amplifies the dimer population up to ~75%, where a plateau-level is achieved, without change of compactness, as evidenced by the Kratky plot in Figure S3 in the S.I. The switch from monomers to a mixture of monomers and dimers after binding, in both dark and light conditions, is also

evidenced by the much larger values (nearly double) of the radius of gyration, R_g , and of the scattering intensity, $I(0)$, obtained by Guinier analysis⁴⁹ (Figure 3c). This result is further supported by the Porod-invariant method, which is model-independent, used to calculate the molecular volume of the various samples (S.I.).

Due to the higher sensitivity of X-rays to hydration water and ion clouds around DNA,^{51,52} R_g obtained by SAXS are approximately 3 Å higher than the corresponding SANS values (Table S1), which is consistent with the ~2-4 Å offset between SAXS and SANS data already obtained for DNA solutions.⁵²

It is important to underline that despite the different sensitivity of the two techniques,^{51,52} the overall behavior of the percentage of dimers is the same (Figure 3d), validating the fact that X-ray irradiation does not affect the observed structure, and that the process is reproducible. The trend of dimer proportion as a function of irradiation time was fitted with an exponential law, providing the characteristic rising rate of $1/160 \text{ s}^{-1}$ to the plateau-level (Table S2).

Finally, CD was used to characterize, in the same conditions as the SAXS/SANS measurements, the effects of complexation with TMPyP4 and irradiation with blue light on the Tel22 secondary structure. CD data are reported in Figure 4a, revealing that the most striking change occurs at the transition from free to bound form, consistently with what was detected at the larger scale by SAXS/SANS experiments. This is further confirmed by the raising of the induced CD band (iCD) around 440 nm (Figure S5 in the S.I.), assigned to a π - π^* transition of the tetrapyrrole moiety, indicating that TMPyP4 is efficiently interacting with Tel22. Light irradiation then increases this effect, as observed in SAXS/SANS data.

A method based on the principal component and singular value decomposition analysis of a reference spectral library of 23 G-quadruplexes of known structure,⁵³ was used to quantify the

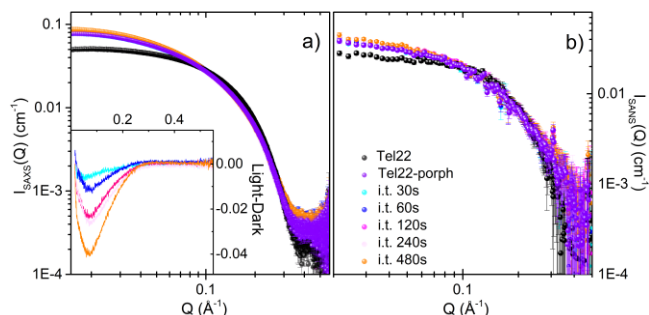


Figure 2. a) SAXS and b) SANS patterns for free Tel22 (black symbols), Tel22 after complexation with TMPyP4 (violet symbols) and after irradiation of the complex with 430 nm light during 30 s (cyan symbols), 60 s (blue symbols), 120 s (magenta symbols), 240 s (pink symbols), and 480 s (orange symbols). The inset enhances the light effect, showing the difference, normalized to $I(0)$, between the irradiated (Light) and the non-irradiated (Dark) Tel22-TMPyP4 SAXS profiles (see also Figure S4).

redistribution of secondary structural elements after binding and exposure to blue light. In particular, the fractions of base steps in *anti-anti*, *syn-anti*, or *anti-syn* conformations, and in diagonal or lateral loops were evaluated. The base segments in double chain-reversal loops or extremal nucleotides that may or may not be piled up onto end quartets were also considered, and hereinafter referred to as *ext*. Figures 4b and 4c show, as an example, the result obtained by constraining least-square fitting of Tel22 CD profile to the principal five secondary basis spectra (see also Figure S6), the corresponding tertiary structure being compatible with a hybrid-type mixed parallel/antiparallel G-quadruplex topology.^{39,54,55} The method was applied to all the solutions. Clearly, the structural features of Tel22-TMPyP4 complexes are affected by irradiation. Interestingly, the difference between dark and light profiles of Tel22-TMPyP4 samples (Figure S7 in the S.I.) recalls the CD spectrum of dTdA oligonucleotide,⁵⁶ suggesting that the external thymines and adenines undergo a post irradiation rearrangement.

The weighting factors of the principal species, used as basis spectra for simulating the experimental profiles, are reported in Table S3 in S.I. for all the samples. A correlation/anticorrelation between the population of dimeric Tel22 and that of *ext/syn-anti* secondary structures obtained from SAXS and CD analysis, respectively, emerges from our data (see Figure 5). Remarkably, the linear trend in the secondary vs quaternary (SQ) correlation plot (dashed line in Figure 5) does not intercept the point of Tel22 monomer. The variation in the *syn-anti* and *ext* fractions upon Tel22-TMPyP4 complexation (~0.5% and ~4%, respectively) corresponds to ~60% change in the Tel22 dimer fraction, while roughly the same modification upon light irradiation corresponds to only a ~20% change. This result indicates that the contribution of secondary structural adjustments on the stabilization of dimers is not the same upon complexation and upon light irradiation.

Both the large Soret band red-shift and the pronounced hypochromic effect in UV-VIS spectra^{44,45} hint that, under our experimental conditions, porphyrin interacts with Tel22 *via* stacking on terminal guanines or intercalation, favoring the formation of oblong scaffolds, while excluding interaction *via* external grooves, which would result in a lower red-shift (< 8 nm) and a lower hypochromic effect (<10 %).⁵⁷ Once complexation occurs, light irradiation gives rise to other structural rearrangements which further promote Tel22 dimeric state up to a value of ~ 75% as revealed by the SQ plot in Figure 5: as the portion of dimers increases, the *ext* contribution increases, whereas the *syn-anti* species decreases. Indeed, the former population, mainly referring to terminal nucleotides, is affected by irradiation and is likely to be strongly involved in the intermolecular contacts stabilizing dimers. Conversely, the *syn-anti* fraction diminishes, probably due to the distortion or breaking of the quartets on the external tetrads, giving rise to a larger population of elongated forms. To shed more light on how the binding of TMPyP4 can cause

changes in the *syn-anti* and *ext* portions of the quadruplex scaffold the idea is to use in the near future parallel-stranded G4s with all anti glycosidic bonds.^{7,8,42,53}

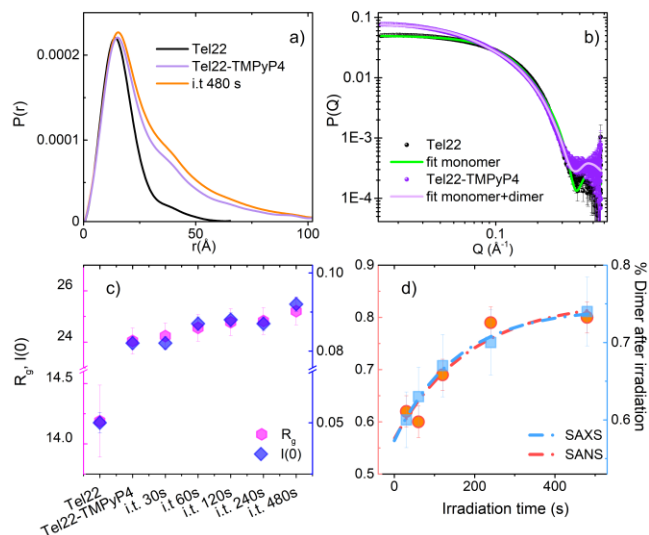


Figure 3. Structural information from SAXS. a) $P(r)$ functions calculated from SAXS data for free Tel22 ($D_{\max}=65$ Å), the Tel22-TMPyP4 complex ($D_{\max}=108$ Å) and after irradiation of the complex during 480 s ($D_{\max}=110$ Å). b) Experimental and theoretical SAXS profiles for Tel22 and Tel22-TMPyP4. The patterns of Tel22 are finely reproduced in terms of a cylindrical form factor compatible with the size of a Tel22 monomer; the Tel22-TMPyP4 form factor is described by a mixture of monomers and dimers. c) R_g and $I(0)$, obtained by the Guinier analysis, and d) percentage of dimers for the Tel22-TMPyP4 complex after irradiation at 430 nm during different exposure times (dashed lines reproduce the exponential growth of the amount of dimers with a saturation characteristic rate in agreement with the model-free analysis results reported in the S.I.).

An interaction occurring along the longitudinal axis rather than laterally is further confirmed by the SAXS results: dimer longer axis is about 80 Å (vs. monomer ~ 36 Å), suggesting that porphyrin molecules occupy a certain space (tetrads spacing enabling intercalation is about 6.4 Å²²) thus forming elongated complexes.

Altogether, our results point to a mechanism where Tel22-TMPyP4 complexation drives Tel22 dimerization in the dark state, while light-induced secondary structural changes contribute to

further increase Tel22 dimer population. In particular: i) Tel22 complexation with TMPyP4 involves multiple binding sites (i.e by stacking and/or intercalation),^{24,45} and favors up to ~60% Tel22 dimerization (analogous to what observed for other drugs^{38,39}); ii) irradiation with blue light, most likely through the oxidation of the external guanines, would induce the separation of some extremal parts which allows the formation of elongated structures presenting approximately the same size as the non-irradiated dimers, bringing the dimer population up to ~80%.

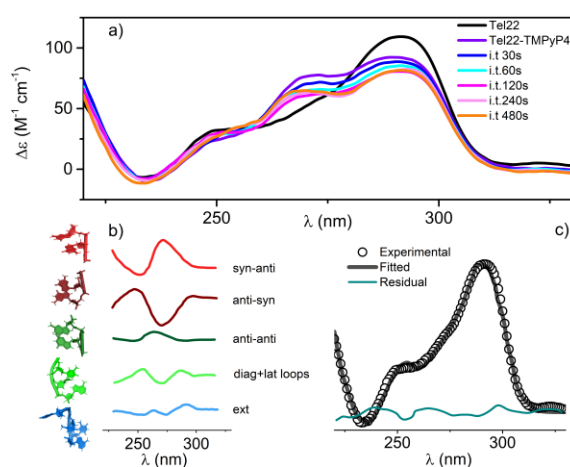


Figure 4. Secondary structure from CD spectroscopy; a) CD signals of free and bound Tel22; irradiated Tel22-TMPyP4 CD spectra are also reported at the indicated exposure times; b) basis spectra used to deconvolve experimental CD profiles; c) experimental CD spectrum and theoretical reconstruction for Tel22.

In conclusion, our study performed using biophysical tools and concepts revealed porphyrin-induced Tel22 dimerization that is further enhanced upon light irradiation. Interestingly, the correlation-plot between secondary and quaternary structural parameters (Figure 5), opens the possibility to *control* and *predict* the fraction of dimers produced during the whole process. Such control and prediction could be improved by using porphyrin derivatives of increased G4s affinity⁵⁸ to optimize the percentage of dimers created. Furthermore, the validity of the SQ plot

can be tested on ligands acting at the cleft of two quadruplex sequences, causing the dimerization of G4s within long telomeric repeats that are of strategic relevance in biology.⁵⁹

Finally, as a future perspective, the combined use of information at different structure-levels will represent a diagnostic strategy to implement the photocontrol of G4 dimerization and stabilization, enabling to tune the telomerase activity in cancer cells. The strict correlation that we found can also be directly employed for tailoring DNA bricks of nanometric size^{60,61,62} for light-switching reversible applications,⁶³ biosensing technologies and nanomedicine design.

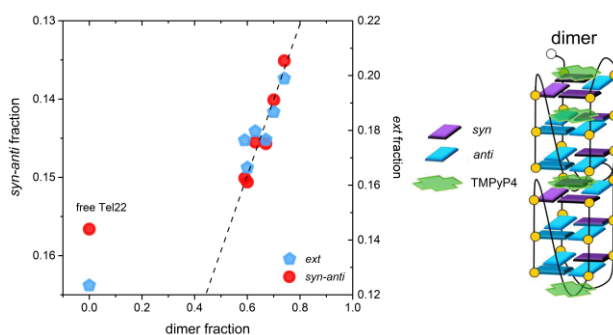


Figure 5. Secondary/Quaternary correlation-plot. Fractions of *syn-anti* secondary structure (circles, left axis) and *ext* secondary structure (diamonds, right axis) obtained by CD spectra analysis as a function of the fraction of Tel22 dimers obtained by X-ray pattern analysis (see main text). A qualitative cartoon representing the dimer-scaffold formed upon complexation is reported on the right.

ASSOCIATED CONTENT

Supporting Information. Materials and Methods are detailed in the S.I. PDF file. The contents of the S.I. are: Materials. Irradiation set-up. Small angle scattering experiments. The Porod Invariant. Model-free analysis of SAXS and SANS patterns. Circular dichroism. CD spectra data analysis.

AUTHOR INFORMATION

The authors declare no competing financial interests.

ACKNOWLEDGMENT

The authors kindly acknowledge Prof. J.B. Chaires and Prof. J.O. Trent for providing the script⁵³ to analyze CD spectra. L.C. and G.S. have received support from CNR- Short Term Mobility (STM) Program. The SOLEIL synchrotron is gratefully acknowledged for access to SWING beamline (proposal 20181022).

REFERENCES

- (1) Spiegel, J.; Adhikari, S.; Balasubramanian, S. The Structure and Function of DNA G-Quadruplexes. *Trends in Chemistry* **2020**, *2* (2), 123–136.
- (2) Hänsel-Hertsch, R.; Di Antonio, M.; Balasubramanian, S. DNA G-Quadruplexes in the Human Genome: Detection, Functions and Therapeutic Potential. *Nat. Rev. Mol. Cell Biol.* **2017**, *18* (5), 279–284.
- (3) Burge, S.; Parkinson, G. N.; Hazel, P.; Todd, A. K.; Neidle, S. Quadruplex DNA: Sequence, Topology and Structure. *Nucleic Acids Research* **2006**, *34* (19), 5402–5415.
- (4) Chen, Y.; Yang, D. Sequence, Stability, and Structure of G-Quadruplexes and Their Interactions with Drugs. *Curr. Protoc. Nucleic Acid Chem.* **2012**, Chapter 17, Unit 17.5.
- (5) Simonsson, T. G-Quadruplex DNA Structures Variations on a Theme. *Biological Chemistry* **2001**, *382* (4), 621–8.
- (6) Karsisiotis, A. I.; O’Kane, C.; da Silva, M. W. DNA Quadruplex Folding Formalism – A Tutorial on Quadruplex Topologies. *Methods* **2013**, *64* (1), 28–35.
- (7) Dvorkin, S. A.; Karsisiotis, A. I.; Webba da Silva, M. Encoding Canonical DNA Quadruplex Structure. *Sci. Adv.* **2018**, *4* (8), eaat3007.
- (8) Karsisiotis, A. I.; Hessari, N. M.; Novellino, E.; Spada, G. P.; Randazzo, A.; Webba da Silva, M. Topological Characterization of Nucleic Acid G-Quadruplexes by UV Absorption and Circular Dichroism. *Angew. Chem. Int. Ed Engl.* **2011**, *50* (45), 10645–10648.
- (9) Reddy Sannapureddi, R. K.; Mohanty, M. K.; Gautam, A. K.; Sathyamoorthy, B. Characterization of DNA G-Quadruplex Topologies with NMR Chemical Shifts. *J. Phys. Chem. Lett.* **2020**, *11* (23), 10016–10022.
- (10) Gray, R. D.; Trent, J. O.; Arumugam, S.; Chaires, J. B. Folding Landscape of a Parallel G-Quadruplex. *J. Phys. Chem. Lett.* **2019**, *10* (5), 1146–1151.
- (11) Tam, D. Y.; Leung, H. M.; Chan, M. S.; Lo, P. K. G-Quadruplex-Mediated Molecular Switching of Self-Assembled 3D DNA. Nanocages. *ChemNanoMat* **2017**, *3* (10), 750–754.
- (12) He, H.-Z.; Chan, D. S.-H.; Leung, C.-H.; Ma, D.-L. G-Quadruplexes for Luminescent Sensing and Logic Gates. *Nucleic Acids Res.* **2013**, *41* (8), 4345–4359.
- (13) Biffi, G.; Tannahill, D.; McCafferty, J.; Balasubramanian, S. Quantitative Visualization of DNA G-

- Quadruplex Structures in Human Cells. *Nat. Chem.* **2013**, *5* (3), 182–186.
- (14) Rhodes, D.; Lipps, H. J. G-Quadruplexes and Their Regulatory Roles in Biology. *Nucleic Acids Res.* **2015**, *43* (18), 8627–8637.
- (15) De Cian, A.; Lacroix, L.; Douarre, C.; Temime-Smaali, N.; Trentesaux, C.; Riou, J.-F.; Mergny, J.-L. Targeting Telomeres and Telomerase. *Biochimie* **2008**, *90* (1), 131–155.
- (16) Sun, D.; Thompson, B.; Cathers, B. E.; Salazar, M.; Kerwin, S. M.; Trent, J. O.; Jenkins, T. C.; Neidle, S.; Hurley, L. H. Inhibition of Human Telomerase by a G-Quadruplex-Interactive Compound. *J. Med. Chem.* **1997**, *40* (14), 2113–2116.
- (17) Jansson, L. I.; Hentschel, J.; Parks, J. W.; Chang, T. R.; Lu, C.; Baral, R.; Bagshaw, C. R.; Stone, M. D. Telomere DNA G-Quadruplex Folding within Actively Extending Human Telomerase. *Proc. Natl. Acad. Sci. U. S. A.* **2019**, *116* (19), 9350–9359.
- (18) Avagliano, D.; Tkaczyk, S.; Sánchez-Murcia, P. A.; González, L. Enhanced Rigidity Changes Ultraviolet Absorption: Effect of a Merocyanine Binder on G-Quadruplex Photophysics. *J. Phys. Chem. Lett.* **2020**, *11* (23), 10212–10218.
- (19) Balasubramanian, S.; Hurley, L. H.; Neidle, S. Targeting G-Quadruplexes in Gene Promoters: A Novel Anticancer Strategy? *Nat. Rev. Drug Discov.* **2011**, *10* (4), 261–275.
- (20) Monchaud, D.; Granzhan, A.; Saettel, N.; Guédin, A.; Mergny, J.-L.; Teulade-Fichou, M.-P. “One Ring to Bind Them All”-Part I: The Efficiency of the Macrocyclic Scaffold for G-Quadruplex DNA Recognition. *J. Nucleic Acids* **2010**, DOI: 10.4061/2010/525862.
- (21) Parkinson, G. N.; Ghosh, R.; Neidle, S. Structural Basis for Binding of Porphyrin to Human Telomeres. *Biochemistry* **2007**, *46* (9), 2390–2397.
- (22) Han, F. X.; Wheelhouse, R. T.; Hurley, L. H. Interactions of TMPyP4 and TMPyP2 with Quadruplex DNA. Structural Basis for the Differential Effects on Telomerase Inhibition. *Journal of the American Chemical Society* **1999**, *121* (15), 3561–3570.
- (23) Wheelhouse, R. T.; Sun, D.; Han, H.; Han, F. X.; Hurley, L. H. Cationic Porphyrins as Telomerase Inhibitors: The Interaction of Tetra-(N-Methyl-4-Pyridyl)porphine with Quadruplex DNA. *Journal of the American Chemical Society* **1998**, *120* (13), 3261–3262.
- (24) Han, H.; Langley, D. R.; Rangan, A.; Hurley, L. H. Selective Interactions of Cationic Porphyrins with G-Quadruplex Structures. *Journal of the American Chemical Society* **2001**, *123* (37), 8902–8913.
- (25) Izbicka, E.; Wheelhouse, R. T.; Raymond, E.; Davidson, K. K.; Lawrence, R. A.; Sun, D.; Windle, B. E.; Hurley, L. H.; Von Hoff, D. D. Effects of Cationic Porphyrins as G-Quadruplex Interactive Agents in Human Tumor Cells. *Cancer Res.* **1999**, *59* (3), 639–644.
- (26) Guo, K.; Gokhale, V.; Hurley, L. H.; Sun, D. Intramolecularly Folded G-Quadruplex and I-Motif Structures in the Proximal Promoter of the Vascular Endothelial Growth Factor Gene. *Nucleic Acids Res.* **2008**, *36* (14), 4598–4608.
- (27) Qin, Y.; Rezler, E. M.; Gokhale, V.; Sun, D.; Hurley, L. H. Characterization of the G-Quadruplexes in the Duplex Nuclease Hypersensitive Element of the PDGF-A Promoter and Modulation of PDGF-A Promoter Activity by TMPyP4. *Nucleic Acids Res.* **2007**, *35* (22), 7698–7713.
- (28) Gunaratnam, M.; Swank, S.; Haider, S. M.; Galesa, K.; Reszka, A. P.; Beltran, M.; Cuenca, F.; Fletcher, J. A.; Neidle, S. Targeting Human Gastrointestinal Stromal Tumor Cells with a Quadruplex-Binding Small Molecule. *J. Med. Chem.* **2009**, *52* (12), 3774–3783.
- (29) Mikami-Terao, Y.; Akiyama, M.; Yuza, Y.; Yanagisawa, T.; Yamada, O.; Yamada, H. Antitumor Activity of G-Quadruplex-Interactive Agent TMPyP4 in K562 Leukemic Cells. *Cancer Lett.* **2008**, *261* (2), 226–234.
- (30) Bonnett, R. Photosensitizers of the Porphyrin and Phthalocyanine Series for Photodynamic Therapy. *Chem. Soc. Rev.*, **1995**, *24*, 19–33.
- (31) Celli, J. P.; Spring, B. Q.; Rizvi, I.; Evans, C. L.; Samkoe, K. S.; Verma, S.; Pogue, B. W.; Hasan, T. Imaging and Photodynamic Therapy: Mechanisms, Monitoring, and Optimization. *Chem. Rev.* **2010**, *110* (5), 2795–2838.
- (32) Lin, Y.; Zhou, T.; Bai, R.; Xie, Y. Chemical Approaches for the Enhancement of Porphyrin Skeleton-Based Photodynamic Therapy. *J. Enzyme Inhib. Med. Chem.* **2020**, *35* (1), 1080–1099.

- (33) Fleming, A. M.; Burrows, C. J. G-Quadruplex Folds of the Human Telomere Sequence Alter the Site Reactivity and Reaction Pathway of Guanine Oxidation Compared to Duplex DNA. *Chemical Research in Toxicology* **2013**, *26*(4), 593-607.
- (34) Beniaminov, A. D.; Novikov, R. A.; Mamaeva, O. K.; Mitkevich, V. A.; Smirnov, I. P.; Livshits, M. A.; Shchvolkina, A. K.; Kaluzhny, D. N. Light-Induced Oxidation of the Telomeric G4 DNA in Complex with Zn(II) Tetracarboxymethyl Porphyrin. *Nucleic Acids Res.* **2016**, *44* (21), 10031–10041.
- (35) Cheng, M.; Cui, Y.-X.; Wang, J.; Zhang, J.; Zhu, L.-N.; Kong, D.-M. G-Quadruplex/Porphyrin Composite Photosensitizer: A Facile Way to Promote Absorption Redshift and Photodynamic Therapy Efficacy. *ACS Appl. Mater. Interfaces* **2019**, *11* (14), 13158–13167.
- (36) Bao, H.-L.; Liu, H.-S.; Xu, Y. Hybrid-Type and Two-Tetrad Antiparallel Telomere DNA G-Quadruplex Structures in Living Human Cells. *Nucleic Acids Research* **2019**, *47* (10), 4940–4947.
- (37) Ambrus, A.; Chen, D.; Dai, J.; Bialis, T.; Jones, R. A.; Yang, D. Human Telomeric Sequence Forms a Hybrid-Type Intramolecular G-Quadruplex Structure with Mixed Parallel/antiparallel Strands in Potassium Solution. *Nucleic Acids Research* **2006**, *34* (9), 2723–2735.
- (38) Bianchi, F.; Comez, L.; Biehl, R.; D'Amico, F.; Gessini, A.; Longo, M.; Masciovecchio, C.; Petrillo, C.; Radulescu, A.; Rossi, B.; Sacchetti, F.; Sebastiani, F.; Violini, N.; Paciaroni, A. Structure of Human Telomere G-Quadruplex in the Presence of a Model Drug along the Thermal Unfolding Pathway. *Nucleic Acids Research* **2018**, *46*(22), 11927-11938
- (39) Comez, L.; Bianchi, F.; Libera, V.; Longo, M.; Petrillo, C.; Sacchetti, F.; Sebastiani, F.; D'Amico, F.; Rossi, B.; Gessini, A.; Masciovecchio, C.; Amenitsch, H.; Sissi, C.; Paciaroni, A. Polymorphism of Human Telomeric Quadruplexes with Drugs: A Multi-Technique Biophysical Study. *Phys. Chem. Chem. Phys.* **2020**, *22* (20), 11583–11592.
- (40) Gabelica, V.; Baker, E. S.; Teulade-Fichou, M.-P.; De Pauw, E.; Bowers, M. T. Stabilization and Structure of Telomeric and c-Myc Region Intramolecular G-Quadruplexes: The Role of Central Cations and Small Planar Ligands. *J. Am. Chem. Soc.* **2007**, *129* (4), 895–904.
- (41) Alcaro, S.; Musetti, C.; Distinto, S.; Casatti, M.; Zagotto, G.; Artese, A.; Parrotta, L.; Moraca, F.; Costa, G.; Ortuso, F.; Maccioni, E.; Sissi, C. Identification and Characterization of New DNA G-Quadruplex Binders Selected by a Combination of Ligand and Structure-Based Virtual Screening Approaches. *J. Med. Chem.* **2013**, *56* (3), 843–855.
- (42) Renčiuk, D.; Kejnovská, I.; Školáková, P.; Bednářová, K.; Motlová, J.; Vorlíčková, M. Arrangements of Human Telomere DNA Quadruplex in Physiologically Relevant K Solutions. *Nucleic Acids Research* **2009**, *37* (19) 6625–6634.
- (43) Marchand, A.; Granzhan, A.; Iida, K.; Tsushima, Y.; Ma, Y.; Nagasawa, K.; Teulade-Fichou, M.-P.; Gabelica, V. Ligand-Induced Conformational Changes with Cation Ejection upon Binding to Human Telomeric DNA G-Quadruplexes. *J. Am. Chem. Soc.* **2015**, *137* (2), 750–756.
- (44) Anantha, N. V.; Azam, M.; Sheardy, R. D. Porphyrin Binding to Quadruplexed T4G4. *Biochemistry* **1998**, *37* (9), 2709–2714.
- (45) Wei, C.; Jia, G.; Yuan, J.; Feng, Z.; Li, C. A Spectroscopic Study on the Interactions of Porphyrin with G-Quadruplex DNAs. *Biochemistry* **2006**, *45* (21), 6681–6691.
- (46) Svergun, D. I. Determination of the Regularization Parameter in Indirect-Transform Methods Using Perceptual Criteria. *Journal of Applied Crystallography* **1992**, *25*, 495-503.
- (47) Parkinson, G. N.; Lee, M. P. H.; Neidle, S. Crystal Structure of Parallel Quadruplexes from Human Telomeric DNA. *Nature* **2002**, *417* (6891), 876–880.
- (48) Phan, A. T.; Kuryavyi, V.; Gaw, H. Y.; Patel, D. J. Small-Molecule Interaction with a Five-Guanine-Tract G-Quadruplex Structure from the Human MYC Promoter. *Nat. Chem. Biol.* **2005**, *1* (3), 167–173.
- (49) Mariani, P.; Spinozzi, F.; Federiconi, F.; Ortore, M. G.; Amenitsch, H.; Spindler, L.; Drevensek-Olenik, I. Guanosine Quadruplexes in Solution: A Small-Angle X-Ray Scattering Analysis of Temperature Effects on Self-Assembling of Deoxyguanosine Monophosphate. *J. Nucleic Acids* **2010**, DOI: 10.4061/2010/472478.
- (50) Monsen, R. C.; Chakravarthy, S.; Dean, W. L.; Chaires, J. B.; Trent, J. O. The Solution Structures of

- Higher-Order Human Telomere G-Quadruplex Multimers. *Nucleic Acids Res.* **2021**, *49* (3), 1749–1768.
- (51) Meisburger, S. P.; Pabit, S. A.; Pollack, L. Determining the Locations of Ions and Water around DNA from X-Ray Scattering Measurements. *Biophys. J.* **2015**, *108* (12), 2886–2895.
- (52) Andresen, K.; Das, R.; Park, H. Y.; Smith, H.; Kwok, L. W.; Lamb, J. S.; Kirkland, E. J.; Herschlag, D.; Finkelstein, K. D.; Pollack, L. Spatial Distribution of Competing Ions around DNA in Solution. *Phys. Rev. Lett.* **2004**, *93* (24), 248103.
- (53) del Villar-Guerra, R.; Trent, J. O.; Chaires, J. B. G-Quadruplex Secondary Structure Obtained from Circular Dichroism Spectroscopy. *Angew. Chem. Int. Ed Engl.* **2018**, *130* (24), 7289–7293.
- (54) Wang, Y.; Patel, D. J. Solution structure of the human telomeric repeat d[AG₃(T₂AG₃)₃] G-tetraplex. *Structure* **1993**, *1* (4) 263-282.
- (55) Luu, K. N.; Phan, A. T.; Kuryavyi, V.; Lacroix, L.; Patel, D. J. Structure of the Human Telomere in K Solution: An Intramolecular (3+1) G-Quadruplex Scaffold. *J. Am. Chem. Soc.* **2006**, *128* (30), 9963–9970.
- (56) Cantor, C. R.; Warshaw, M. M.; Shapiro, H. Oligonucleotide Interactions. Circular Dichroism Studies of the Conformation of Deoxyoligonucleotides. *Biopolymers* **1970**, *9* (9), 1059–1077.
- (57) Pasternack, R. F.; Gibbs, E. J.; Villafranca, J. J. Interactions of Porphyrins with Nucleic Acids. *Biochemistry* **1983**, *22* (10), 2406-2414
- (58) Boschi, E.; Davis, E.; Taylor, S.; Butterworth, A.; Chirayath, L. A.; Purohit, V.; Siegel, L. K.; Buenaventura, J.; Sheriff, A. H.; Jin, R.; Sheardy, R.; Yatsunyk, L. A.; Azam, M. Interaction of a Cationic Porphyrin and Its Metal Derivatives with G-Quadruplex DNA. *The Journal of Physical Chemistry B* **2016**, *120* (50), 12807–12819.
- (59) Zhao, C.; Wu, L.; Ren, J.; Xu, Y.; Qu, X. Targeting Human Telomeric Higher-Order DNA: Dimeric G-Quadruplex Units Serve as Preferred Binding Site. *J. Am. Chem. Soc.* **2013**, *135* (50), 18786–18789.
- (60) Tian, T.; Song, Y.; Wei, L.; Wang, J.; Fu, B.; He, Z.; Yang, X.-R.; Wu, F.; Xu, G.; Liu, S.-M.; Li, C.; Wang, S.; Zhou, X. Reversible Manipulation of the G-Quadruplex Structures and Enzymatic Reactions through Supramolecular Host-Guest Interactions. *Nucleic Acids Res.* **2017**, *45* (5), 2283–2293.
- (61) Ma, D.-L.; Zhang, Z.; Wang, M.; Lu, L.; Zhong, H.-J.; Leung, C.-H. Recent Developments in G-Quadruplex Probes. *Chem. Biol.* **2015**, *22* (7), 812–828.
- (62) Nishio, M.; Tsukakoshi, K.; Ikebukuro, K. G-Quadruplex: Flexible Conformational Changes by Cations, pH, Crowding and Its Applications to Biosensing. *Biosens. Bioelectron.* **2021**, *178*, 113030.
- (63) O'Hagan, M. P.; Haldar, S.; Duchi, M.; Oliver, T. A. A.; Mulholland, A. J.; Morales, J. C.; Carmen Galan, M. C. A Photoresponsive Stiff-Stilbene Ligand Fuels the Reversible Unfolding of G-Quadruplex DNA. *Angew. Chem. Int. Ed Engl.* **2019**, *58* (13) 4334–38.